



Cite this: *Chem. Commun.*, 2023, 59, 7399

Received 11th April 2023,  
Accepted 8th May 2023

DOI: 10.1039/d3cc01769a

[rsc.li/chemcomm](http://rsc.li/chemcomm)

**A novel dansyl-triazole-based fluorescent macrocycle with high Stokes shift and positive solvatochromism was developed. This is an excellent fluorescence sensor for selective detection of nitro-containing antibiotics and other nitro-heteroaromatics. Detection was possible in real samples/paper strips in submicromolar concentration. The interaction of the macrocycle with multiple proteins exhibited its bioactivity.**

Macrocycles have been a fascinating class of molecules for over five decades due to their artful synthesis, exceptional properties, and wide applications in the fields of material and biomedical research. Macrocycles are advantageous in host-guest chemistry as their entropy penalty during binding is comparatively less due to their preorganized conformation and limited flexibility.<sup>1</sup> Cyclodextrin, cucurbit[n]uril, calix[n]arenes, pillar[n]arenes, etc., are well-known macrocyclic host molecules<sup>2</sup> which are highly efficient for molecular recognition that occurs due to secondary interactions or non-covalent bonding with other proteins, ions, or other small molecules. They have been extensively exploited for binding various analytes, and organic fluorescent dyes are among the most studied guests.<sup>3</sup> However, the detection of binding of non-fluorescent analytes is challenging in these classes of macrocycles, or it is possible only when a fluorophore dye is first bound, leading to a competitiveness in binding in the presence of a secondary analyte. Thus, fluorescent active macrocycles are in high demand due to their potential to act as effective sensors for various analytes including biomolecules, environmental pollutants, drugs, metals, and other small molecules. In addition, they can also be used as probes to track various analytes in living systems as well as for cellular imaging.

Covalently linking a fluorophore on the backbone or side-chain of macrocycles with reactive binding motifs can be employed to detect fluorescent-silent analytes. Bimane,<sup>4</sup> dansyl,<sup>5</sup> dabsyl,<sup>6</sup> Alexa Fluor,<sup>7</sup> Alexa adamantane,<sup>8</sup> rhodamine,<sup>9</sup>

curcumin<sup>10</sup> etc. are a few of the fluorophores linked with macrocycles in various reports. The dansyl group is a highly promising fluorophore which shows a good fluorescence emission and thus has been used to link with various important moieties such as proteins,<sup>11</sup> amino acids,<sup>12</sup> antibodies,<sup>13</sup> sensor molecules<sup>14,15</sup> and so on. Copper-catalyzed alkyne-azide click reaction was used as the macrocyclization strategy. The triazole formed after the reaction has been reported to have extensive functional properties and applications in various materials and biomedical research.<sup>16</sup>

Aza-oxa-triazole-based functionally tunable macrocycles were reported to interact well with different proteins.<sup>17</sup> Appending a fluorophore like a dansyl on such macrocycles can lead to a good interaction with proteins; at the same time, the fluorescence emission property can be employed for sensing or detection of various analytes. In this report, we synthesized a dansyl-appended fluorescent aza-oxa-triazole-based macrocycle for the detection of nitro-containing drugs. Nitro-containing drugs are used for treatment processes in aquaculture and can easily enter into water resources and food chains because of their low degradation level.<sup>18</sup> So, a sensor for the selective detection of these drugs from water and other sources will be extremely useful, and our newly developed dansyl-triazole macrocycle (DTMC) serves this purpose. At the same time, bioactivity and interactions with proteins are extremely important for the use of this system as host molecule in biological samples *in vivo* and *in vitro* and this study has also been performed with DTMC.

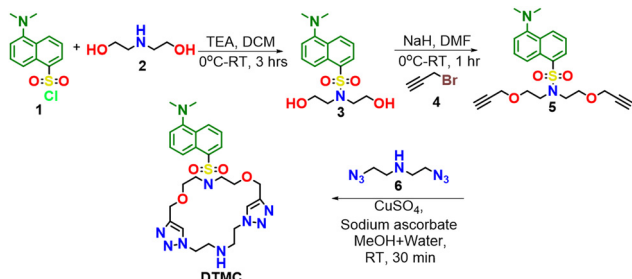
The strategy for synthesizing the macrocycle was made as simple as possible. A dialkyne derivative and diazide derivative were synthesized separately and clicked using a copper-catalyzed azide-alkyne click reaction to form the macrocycle. The fluorophore dansyl was attached to the alkyne part by a two-step reaction. In the first step, dansyl chloride (1, Scheme 1) was reacted with diethanolamine (2, Scheme 1) in the presence of base triethylamine. After extraction, the product (3, Scheme 1) was directly used for propargylation by using propargyl bromide in the presence of a strong base, sodium hydride, to result in the dialkyne (5, Scheme 1) for the click reaction. The diazide (6, Scheme 1) was synthesized as per a previously reported procedure.<sup>19</sup> Macrocyclization is the most crucial step in the whole synthesis of a macrocycle. The

<sup>a</sup> Department of Chemistry, Indian Institute of Technology Palakkad, Kerala 678557, India. E-mail: mintu@iitpkd.ac.in

<sup>b</sup> Environmental Sciences and Sustainable Engineering Centre, Indian Institute of Technology Palakkad, Kerala 678557, India

† Electronic supplementary information (ESI) available. See DOI: <https://doi.org/10.1039/d3cc01769a>





Scheme 1 Synthesis of the dansyl-triazole-based macrocycle (DTMC).

macrocyclization employed here by the click reaction of a dialkyne and a diazide is a bimolecular heterodifunctional approach.

Here, we performed the click reaction for macrocycle formation by using CuSO<sub>4</sub> with sodium L-ascorbate in a solvent of water and methanol, completed in half an hour. The product obtained was characterized by liquid chromatography-mass spectrometry (LC-MS) (Fig. 1a and Fig. S10, S11, ESI<sup>†</sup>), infrared (IR) spectroscopy (Fig. 1b and Fig. S12, ESI<sup>†</sup>), <sup>1</sup>H nuclear magnetic resonance (NMR) spectroscopy (Fig. 1c and Fig. S13, ESI<sup>†</sup>) and <sup>13</sup>C NMR spectroscopy (Fig. S14, ESI<sup>†</sup>). The expected mass ([M+H]<sup>+</sup>) of the product DTMC was 570.25 Da, and we observed [M+H]<sup>+</sup> at 570.40 Da. In the IR spectrum, the peaks for the stretching frequency of  $\text{N}=\text{N}-\text{N}-$  and  $\text{C}=\text{C}$  of the triazole were observed at  $2102\text{ cm}^{-1}$  and  $1705\text{ cm}^{-1}$ , respectively. This confirmed the formation of the triazole ring. The <sup>1</sup>H NMR and <sup>13</sup>C NMR spectra also showed the peaks corresponding to all hydrogens and carbons present in DTMC.

A study on the photophysical properties of the synthesized macrocycle DTMC was carried out by monitoring various parameters. The absorption spectrum of DTMC was recorded, and the

maximum wavelength was observed at 332 nm. The emission was recorded, and  $\lambda_{\text{max}}$  was observed at 567 nm, resulting in a very high Stokes shift ( $\Delta\lambda$ ) of 235 nm (Fig. 2a). The overlap between the excitation and emission is very minimal with this molecule. This high Stokes shift makes DTMC highly useful for fluorescence-based sensing and imaging applications, more viable due to the minimum molar self-absorption and self-quenching. Stokes shift at this level is important to achieve a high signal-to-noise ratio for higher-level applications like single-molecule studies.

The emission was also recorded in different solvents, such as hexane, toluene, chloroform, acetone, and dimethyl sulfoxide, and a bathochromic shift of 90 nm from blue (445 nm) to greenish yellow (535 nm) color (Fig. 2b and Fig. S15, ESI<sup>†</sup>) was observed. This positive solvatochromism is because of the stabilization of the excited state of DTMC in the presence of polar solvents, increasing the emission wavelength. At the same time, internal charge transfer (ICT) will also be altered due to neighboring solvents around the fluorophore. The fluorescence quantum yield is a measure of the tendency of a fluorophore to emit light after being excited. This value also suggests the level of fluorescence of a molecule. The quantum yield was calculated for DTMC and a good quantum yield of 0.308 was obtained, which indicates the applicability of this molecule.

A study on the sensing of various pharmaceuticals is of importance because they have become highly prevalent contaminants in water bodies. These pharmaceuticals, at uncontrolled levels, cause deleterious effects on the health of humans and associated animals to a great extent. So, it is imperative to have methods or materials to detect and quantify the presence of these drug molecules in various systems. We selected a few pharmaceutical drugs commonly used for various human and animal treatments, including antibiotics, analgesics, anti-inflammatories, and anti-tuberculosis drugs. The drugs chosen were dimetridazole (DMI), nitrofurantoin (NFT), nitrofurazone (NFZ), sulfamethazine (SMZ), sulfadiazine (SDZ), diclofenac (DCL), mefenamic acid (MFA), pyrazinamide (PZA), and isoniazid (INZ), and the structures of these are given in Fig. S17 (ESI<sup>†</sup>). The interaction of these drugs with the macrocycle DTMC was studied by fluorescence spectroscopy utilizing the high emission property of DTMC at 565 nm. Other analytes like metal salts such as NaCl, KCl, MgSO<sub>4</sub>, and NaHCO<sub>3</sub> and metabolites like glucose, urea, and creatinine were

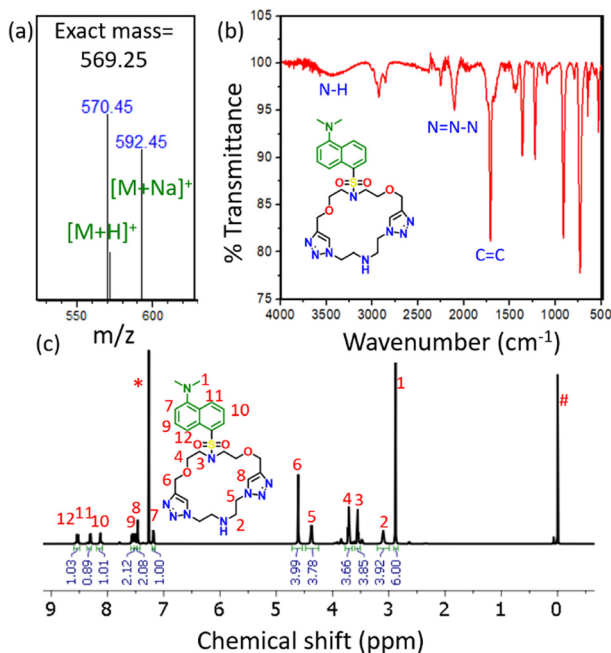


Fig. 1 Spectral characterization of DTMC. (a) Mass spectrum, (b) IR spectrum and (c) <sup>1</sup>H NMR spectrum of DTMC in CDCl<sub>3</sub> ('#' represents the residual peak of internal standard tetramethylsilane, and '\*' represents the residual peak of the solvent CDCl<sub>3</sub>).

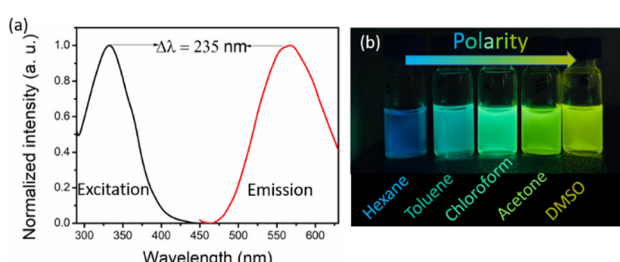


Fig. 2 (a) Excitation-emission spectra of DTMC (10  $\mu\text{M}$  in 0.2% DMSO in water at emission wavelength of 560 nm and excitation wavelength of 330 nm). (b) Photograph showing solvatochromism of DTMC (1 mg  $\text{mL}^{-1}$ ) in various solvents, hexane, toluene, chloroform, acetone, and dimethyl sulfoxide (DMSO), captured under a UV lamp.



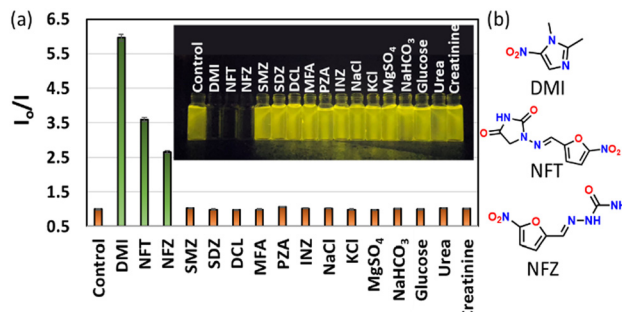


Fig. 3 (a) Selectivity in fluorescence quenching of DTMC ( $10 \mu\text{M}$  in  $0.2\%$  DMSO in water) in the presence of various drugs ( $200 \mu\text{M}$ ) ( $I_0$  is the fluorescence intensity of DTMC alone and  $I$  is the fluorescence intensity in the presence of analyte when excited at  $330 \text{ nm}$ ). Inset: digital photograph of DTMC ( $100 \mu\text{M}$ ) in the presence of various analytes ( $1 \text{ mM}$ ) under UV light. (b) Chemical structures of DMI, NFT, and NFZ, with which DTMC showed an interaction.

also tested. Good quenching of fluorescence was observed for selected drugs such as DMI, followed by NFT, and NFZ, and no appreciable change in the fluorescence intensity was observed with other analytes (Fig. 3a and Fig. S18, ESI<sup>†</sup>). When closely checking the structure of the DTMC-interacting drugs, it was deduced that all three drugs contained a nitro group attached to them. This change was observed in the fluorescence spectrum and visually under UV light. The competitiveness of these three drugs in the presence of other analytes was also studied and it was observed that the quenching was intact even in the presence of other competing drugs, metal salts and metabolites (Fig. S19, ESI<sup>†</sup>).

The three drugs DMI, NFT, and NFZ, which showed an interaction with DTMC, are popularly used as antibiotics. These kinds of medicines are often discharged into waterbodies and make them polluted. The most serious effect lies in bacteria gaining resistance when exposed to a higher level. Thus, sensors like DTMC for the detection of these drugs are advantageous. DTMC showed a very good interaction with the three drugs, as shown in Fig. 4. The binding strength is quantified using the nonlinear Stern–Volmer plot. The Stern–Volmer quenching constant ( $K_{SV}$ ) was also calculated, and it was found that  $K_{SV}$  was highest for DMI ( $13.4 (\pm 1.18) \times 10^3 \text{ M}^{-1}$ ), followed by NFT ( $5.74 (\pm 0.26) \times 10^3 \text{ M}^{-1}$ ) and NFZ ( $4.57 (\pm 0.25) \times 10^3 \text{ M}^{-1}$ ) (Fig. S20, ESI<sup>†</sup>). The limit of detection was observed to be very low in the submicromolar range with the least value for DMI ( $100 \text{ nM}$ ), followed by NFT ( $500 \text{ nM}$ ) and NFZ ( $1 \mu\text{M}$ ).

As the solution-state sensing of the drugs was successful using DTMC, sensing the same in a simpler platform was investigated. Paper strips are a good platform to address this due to their several advantages of lower cost, ease of availability, ease of handling and portability. For the study, Whatman filter papers were cut as strips and DTMC solution dropped on both sides: one as the control and one as the test. Drops of drug solutions were added to the DTMC spot and checked under UV light. We could observe the quenching of fluorescence on the strips easily without any sophisticated instruments in a simple way (Fig. S21, ESI<sup>†</sup>). The stability of these strips was also checked by looking at the level of fluorescence of the same strip after ten days (Fig. S22, ESI<sup>†</sup>). We observed that the strips are stable for more than 10 days and can be stored for long-term use. This increases the practical applicability

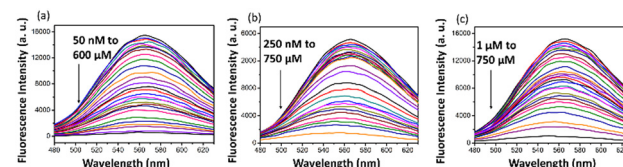


Fig. 4 Fluorescence of DTMC ( $10 \mu\text{M}$  in  $0.2\%$  DMSO in water) at  $25^\circ\text{C}$  upon the addition of different concentrations of (a) DMI, (b) NFT and (c) NFZ when excited at  $330 \text{ nm}$ .

of DTMC as a sensor for DMI, NFT, and NFZ. The sensing property of DTMC against these drugs was intact even in the presence of many contaminants in water samples, like lake water and tap water (Fig. S23, ESI<sup>†</sup>). This quenching of fluorescence reflects the effect of competing contaminants along with the presence of the drugs in sensing. The sensing was also carried out for the trace amounts present in human serum albumin (HSA) to mimic the sensing in body fluid. As DMI is mostly used in animal feed, the presence of the drug in a milk sample was also tested. In all the samples, the fluorescence of DTMC was considerably quenched upon the addition of DMI, NFT, and NFZ (Fig. S22, ESI<sup>†</sup>). Thus, it is well understood that the macrocycle DTMC can be used for the on-spot sensing of the selected drugs for real sensing applications.

When studying the interaction with pharmaceutical agents, it was observed that the only drugs to show selectivity among other drugs were the nitro-containing heteroaromatics. To confirm this selectivity, we carried out the same study with many other nitro-containing compounds like 2-chloro-6-nitrobenzothiazole (CNB), 5-nitroisoquinoline (NIQ), 2-amino-6-nitrobenzothiazole (ANB), 2-mercapto-5-nitrobenzimidazole (MNB), and 2-nitrothiophene (NTP) (Fig. 5a). A very good quenching of DTMC fluorescence was observed by adding any of these compounds, which confirms the role of nitro groups in the quenching of fluorescence (Fig. 5b). We added imidazole and measured the fluorescence intensity to study whether any heterocycle alone can interact with the macrocycle. However, no quenching of fluorescence was observed for imidazole. At the same time, the effect of the nitro group on a non-heteroaromatic system was studied by adding nitrobenzene. Still, the fluorescence intensity remained unaltered. This result confirmed

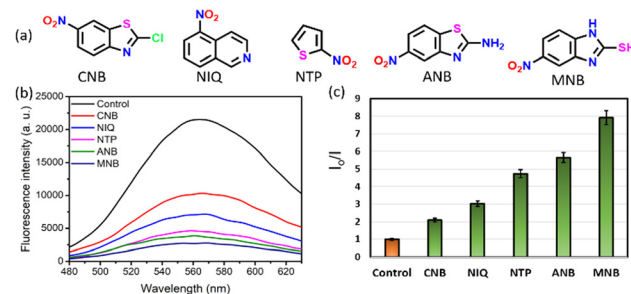


Fig. 5 (a) Chemical structures of nitro-heteroaromatic compounds. (b) Fluorescence spectra of DTMC (control,  $10 \mu\text{M}$  in  $0.2\%$  DMSO in water) upon the addition of various nitro-heteroaromatic compounds ( $200 \mu\text{M}$ ). (c) Bar diagram showing  $I_0/I$  of DTMC upon the addition of various nitro-heteroaromatic compounds ( $I_0$  is the fluorescence intensity of DTMC alone and  $I$  is the fluorescence intensity in the presence of the test compounds at  $25^\circ\text{C}$  when excited at  $330 \text{ nm}$ ).



**Table 1** Stern–Volmer quenching constant calculated from fluorescence spectroscopy and binding energy calculated from molecular docking when DTMC interacted with various proteins

Protein	Stern–Volmer quenching constant ( $K_{SV}$ ), $\times 10^3 \text{ M}^{-1}$	Binding energy (kcal mol $^{-1}$ )
HSA	7.78 $\pm$ 0.13	-10.8
BSA	6.07 $\pm$ 0.08	-9.9
Lysozyme	4.56 $\pm$ 0.19	-7.9
Proteinase	7.24 $\pm$ 0.14	-8.3
Trypsin	5.44 $\pm$ 0.16	-8.1

that DTMC interacts only with nitro-containing heteroaromatic compounds. This result holds the same even when other functional groups like thiol, amino, and chloro are also attached to the ring.

The mechanism for the quenching of fluorescence of DTMC in the presence of nitro-containing heteroaromatics can be explained *via* the following. The fluorescence of the dansyl group alone can be explained due to the ICT or the push–pull mechanism from the electron-rich dimethyl group to the electron-deficient sulfonyl group. When an electron-deficient nitro-group-containing compound was added to the system, the ICT was hindered, and fluorescence quenching was observed. The triazole in the macrocycle can also help in bringing the analyte to its vicinity to make a  $\pi$ – $\pi$  interaction. The  $-\text{NH}-$  group present in the macrocycle can also make a hydrogen bond with the analyte. This combined effect of the dansyl group, triazole groups, and the  $-\text{NH}-$  functional moiety in a preorganized, conformationally stable macrocyclic architecture makes DTMC a good candidate for sensing nitro-heteroaromatics. To get an idea of the conformation, computational modelling was carried out, and the optimized structure of DTMC–drug complexes are given in Fig. S24 (ESI $^\ddagger$ ).

The interactions of DTMC with different important proteins were studied to investigate the bioactivity by utilizing the intrinsic fluorescence of proteins *via* fluorescence spectroscopy. Bovine serum albumin (BSA), human serum albumin (HSA), lysozyme, proteinase, and trypsin were selected as proteins for the study. Quenching of fluorescence was observed with all the proteins when added to DTMC. The extent of quenching was calculated by a Stern–Volmer plot (Fig. S25–S29, ESI $^\ddagger$ ). The protein HSA showed the highest interaction with DTMC with Stern–Volmer quenching constant  $K_{SV} = 7.78 \times 10^3 \text{ M}^{-1}$ , followed by BSA. The quenching constant for BSA was  $6.07 \times 10^3 \text{ M}^{-1}$ . The  $K_{SV}$  for other proteins was also calculated, and the data are given in Table 1. The interactions of the macrocycle with diverse proteins were also studied *in silico* by molecular docking studies, the result of which was consistent with the observation from fluorescence studies. Other proteins also interacted with DTMC with relatively low binding energy (Table 1). The 2D interaction plots showed the different interactions made by DTMC with various amino acids (Fig. S30–S34, ESI $^\ddagger$ ). Thus, this macrocycle is a promising candidate to explore further as a drug delivery vehicle on account of its bioactivity.

In conclusion, a new fluorescent macrocycle was designed and synthesized by attaching a dansyl fluorophore group *via* copper-catalyzed alkyne–azide click reaction. The special design was enabled to make it an aza-oxa-macrocyclic, and a free  $-\text{NH}-$

group was left to post-synthetically modify the macrocycle for other desirable applications. This macrocycle selectively detected nitro-group-containing heteroaromatic drugs with a limit of detection on a submicromolar scale. The sensing was successfully carried out in samples like lake water, tap water, human serum albumin, and milk samples. It was further developed to a paper-strip-based sensor for use in on-site detection of analytes. The bioactivity of the synthesized macrocycle was also explored by studying the interactions with multiple proteins by fluorescence spectroscopy and molecular docking. Both the studies suggested a favorable interaction with proteins, and the results open up applications of DTMC which can be explored in the future as a drug delivery vehicle and so on.

M. P. conceived the concept. M. P. and L. T. conceived the molecular design and synthetic protocols. R. K. M. and L. T. carried out all the experiments. R. K. M., L. T. and M. P. analyzed the data. R. K. M., L. T. and M. P. wrote the paper.

We acknowledge Ramanujan Fellowship (SB/S2/RJN-145/2017), Science and Engineering Research Board, Department of Science and Technology, India; the Core Research Grant (CRG/2019/002495), Science and Engineering Research Board, Department of Science and Technology, India and Scheme for Transformational and Advanced Research in Sciences (MoE/STARS1/293), Ministry of Education and Technology, India for the funding.

## Conflicts of interest

There are no conflicts to declare.

## References

- 1 R. E. Fadler, A. Al Ouahabi, B. Qiao, V. Carta, N. F. Konig, X. Gao, W. Zhao, Y. Zhang, J.-F. Lutz and A. H. Flood, *J. Org. Chem.*, 2021, **86**, 4532–4546.
- 2 Q. Shi, X. Wang, B. Liu, P. Qiao, J. Li and L. Wang, *Chem. Commun.*, 2021, **57**, 12379–12405.
- 3 C. Jiang, Z. Song, L. Yu, S. Ye and H. He, *Trends Anal. Chem.*, 2020, **133**, 116086.
- 4 A. J. Horsfall, K. R. Dunning, K. L. Keeling, D. B. Scanlon, K. L. Wegener and A. D. Abell, *Chem. Bio. Chem.*, 2020, **21**, 3423–3432.
- 5 C. Yang, N. Spinelli, S. Perrier, E. Defrance and E. Peyrin, *Anal. Chem.*, 2015, **87**, 3139–3143.
- 6 O. Hayashida and K. Shibata, *J. Org. Chem.*, 2020, **85**, 5493–5502.
- 7 H. Osaki, C. Chou, M. Taki, K. Welke, D. Yokogawa, S. Irle, Y. Sato, T. Higashiyama, S. Saito and A. Fukazawa, *Angew. Chem.*, 2016, **128**, 7247–7251.
- 8 Z. Liu, W. Lin and Y. Liu, *Acc. Chem. Res.*, 2022, **55**, 3417–3429.
- 9 N. Doumani, E. Bou-Maroun, J. Maalouly, M. Tueni, A. Dubois, C. Bernhard, F. Denat, P. Cayot and N. Sok, *Sensors*, 2019, **19**, 4514.
- 10 M. A. Rankin and B. D. Wagner, *Supramol. Chem.*, 2004, **16**, 513–519.
- 11 M. Suchý, A. Kirby, T. Sabloff, E. E. Mulvihill and A. J. Shuhendler, *New J. Chem.*, 2021, **45**, 13185–13195.
- 12 C. R. Lohani, J. M. Kim and K.-H. Lee, *Tetrahedron*, 2011, **67**, 4130–4136.
- 13 D. Blackmore, Z. Siddiqi, L. Li, N. Wang and W. Maksymowich, *Metabolomics*, 2019, **15**, 1–12.
- 14 Y. Liu, B. Jiang, L. Zhao, L. Zhao, Q. Wang, C. Wang and B. Xu, *Spectrochim. Acta, Part A*, 2021, **261**, 120009.
- 15 A. Jose, R. Sahadevan, M. Vijay, S. Sadhuhan and M. Porel, *Sens. Actuators, B*, 2023, 133335.
- 16 A. K. Agrahari, P. Bose, M. K. Jaiswal, S. Rajkhowa, A. S. Singh, S. Hotha, N. Mishra and V. K. Tiwari, *Chem. Rev.*, 2021, **121**, 7638–7956.
- 17 S. R. Cheekatla, L. Thurakkal, A. Jose, D. Barik and M. Porel, *Molecules*, 2022, **27**, 3409.
- 18 M. Marimuthu, S. S. Arumugam, D. Sabarinathan, H. Li and Q. Chen, *Trends Food Sci. Technol.*, 2021, **116**, 1002–1028.
- 19 J. Románski and P. Jaworski, *Phosphorus, Sulfur Silicon Relat. Elem.*, 2017, **192**, 231–234.

